



Theoretical and experimental study of the vibrational spectra of 1,5-dimethylcytosine

S.A. Brandán^a, G. Benzel^a, J.V. García-Ramos^b,
J.C. Otero^c, A. Ben Altabef^{a,1,*}

^a Instituto de Química Física, Facultad de Bioquímica, Química y Farmacia, Universidad Nacional de Tucumán,
San Lorenzo 456, 4000 Tucumán R., Argentina

^b Instituto de Estructura de la Materia, Consejo Superior de Investigaciones Científicas, Serrano 121, 28006 Madrid, Spain

^c Departamento de Química Física, Facultad de Ciencias, Universidad de Málaga, 29071 Málaga, Spain

Received 30 November 2005; received in revised form 10 October 2007; accepted 5 November 2007

Abstract

The Raman spectra of the solid 1,5-dimethylcytosine and the FTIR spectra at room and low temperatures respectively have been registered. Quantum mechanical calculations of energies, geometries and vibrational wavenumbers were carried out by using *ab initio* (HF) and Density Functional Theory (DFT/BLYP and B3LYP) methods with different basis sets. The best level of theory in order to reproduce the experimental wavenumbers is the BLYP method with the 6-31G* basis set. The theoretical calculations indicate the presence of four stable tautomers of 1,5-dimethylcytosine: amino-oxo; imino-oxo (a and b) and imino-hidroxy. Their geometries were optimised by using the BLYP/6-31G* method, being the amino-oxo tautomer the most stable, followed by the imino-oxo tautomer, while the imino-hidroxy one is the most unstable. The complete assignment of the observed bands in the vibrational spectra of the amino-oxo tautomer is proposed in this work.

© 2007 Published by Elsevier B.V.

Keywords: Infrared; Raman; *ab initio*; DFT; 1,5-Dimethylcytosine

1. Introduction

The vibrational spectroscopy is a very important method for the study of the structure and properties of the biological systems [1–18]. For a few years new research efforts have been made to relate the biological functions of the constituent basis of nucleic acids, DNA and RNA [6–16], with the vibrational properties of uracil, adenine, guanine and cytosine and thiocytosine tautomers, since this relation allows an interpretation of its activity through its physicochemical properties.

DNA methylation plays important roles via regulation of numerous cellular mechanisms in diverse organisms, including humans [19–21]. The methylated derivatives of cytosine [8,11,13] are very interesting due to the fact that the methylation process of a certain sequence of DNA bases can modulate the protein–DNA interaction and consequently

regulate the gene function and the cell differentiation, as reported by Lapinski et al. [13]. For this reason the study of the vibrational spectra of 1,5-dimethylcytosine is very important in biological processes [13,16].

Several spectroscopy studies of cytosine [4,10,12,14] and thiocytosine tautomers [15], 1-methylcytosine [11] and 5-methylcytosine [13,16] have been performed, but only assignments of some bands in the spectra of 1,5-dimethylcytosine in the region between 800 and 100 cm^{−1} have been reported [8]. Moreover, a SERS study of 1,5-dimethylcytosine on Ag or Cu colloids has been reported [17,18].

On the other hand, the vibrational assignments show the probable presence of more than one tautomeric form. It should be observed that in this type of systems it is possible to find different tautomers with similar stabilities and properties. In these cases, the interpretation of the spectra is more complex, especially at low temperatures, due to the overlapping of the bands of different tautomeric forms which complicates the assignment. For this reason it is very useful to have theoretical estimations of the wavenumbers of different tautomeric forms in order to recognize a particular tautomer in the spectra.

* Corresponding author. Tel.: +54 381 4311044; fax: +54 381 4248169.

E-mail address: altabef@fbqf.unt.edu.ar (A. Ben Altabef).

¹ Member of the Carrera del Investigador Científico, CONICET, R. Argentina.

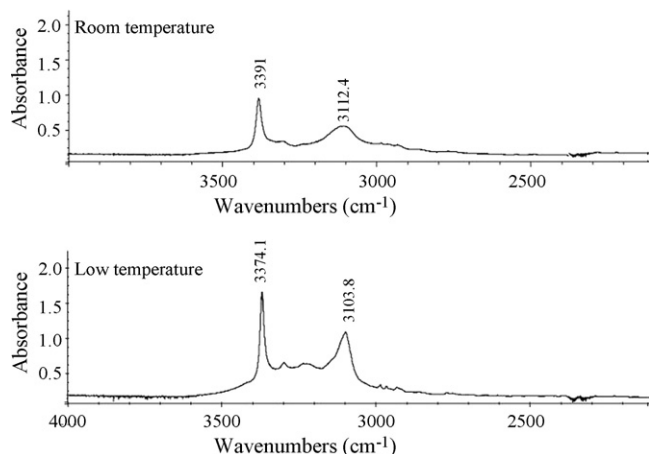


Fig. 1. The IR spectra of solid 1,5-dimethylcytosine at room temperature and at low temperature, between 4000 and 2000 cm⁻¹.

2. Experimental and theoretical calculations

A pure Sigma commercial sample of 1,5-dimethylcytosine was used. The infrared spectra of 1,5-dimethylcytosine at room and low temperatures in KBr pellets, in the range between 4000 and 400 cm⁻¹, were registered on a FTIR PerkinElmer model 1725-X spectrophotometer, equipped with a Globar source and DTGS detector. The infrared spectra at low wavenumbers were registered on a FTIR Digilab model 14 spectrophotometer using polyethylene pellets. Fig. 1 shows the infrared spectra of substance (at room and low temperature (80 K) in a RCII (VLT-2) cell) between 4000 and 2000 cm⁻¹, and Fig. 2 shows the 2000–400 cm⁻¹ region. In addition, the Raman spectra of 1,5-dimethylcytosine were registered in a glass capillary on a Jobin Yvon U-1000 double monochromator spectrometer, using an Ar⁺ laser (Spectra Physics 165, 5145 Å exciting line) (Fig. 3).

All the calculations were made using the Gaussian 98 [22] program package. Geometries and force field calculations were carried out by using *ab initio* (HF) and Density Functional

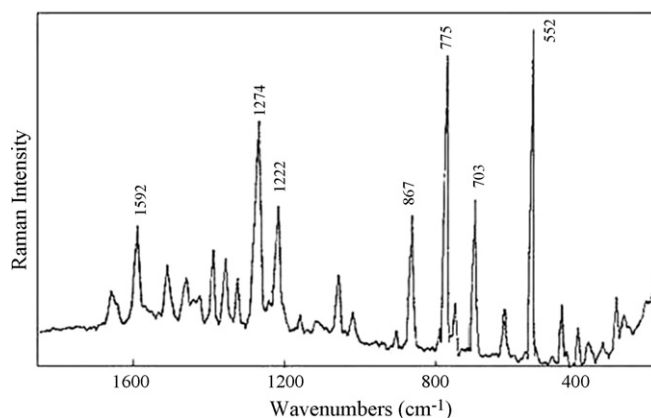


Fig. 3. Raman spectra of solid 1,5-dimethylcytosine.

Theory (DFT, BLYP and B3LYP) methods. The 3-21G, 6-31G, 6-31G*, 6-31G**, 6-31+G, 6-31+G*, 6-311G*, 6-311G**, 6-311+G*, 6-311+G**, 6-311++G** basis sets were used.

3. Results and discussion

From the analysis of the infrared spectra, especially at low temperatures, and the previous results on similar molecules such as cytosine [4,10,12,14] and 5-methylcytosine [13,16], four tautomers of 1,5-dimethylcytosine have been characterised with the aid of theoretical calculations: amino-oxo (I); imino-oxo (IIa); imino-oxo (IIb) and imino-hidroxy (III). The corresponding structures are shown in Fig. 4. Their structures were optimised with different theoretical methods in order to obtain the relative stability, and the respective energies are shown in Table 1. As a result the amino-oxo tautomer is the most stable, followed by the imino-oxo forms; moreover, the imino-hidroxy structure shows a significant larger energy.

Nevertheless, experimental and calculated vibrational wavenumbers of the amino-oxo tautomer have been compared in order to select an adequate level of theory. For this purpose the statistical averages, standard deviations (RMSD) and reliability coefficients, were analysed (Table 2). The BLYP method shows smaller standard deviations and a better reliability coefficient [23] than the B3LYP method, while the HF results are poorer. The 6-31G* basis set shows the best results and diffuse functions produce larger standard deviations. Therefore, the BLYP/6-31G* with smaller RMSD (17.6 cm⁻¹) and better reliability coefficient (0.99) has been selected for the optimisation of the geometry and the force field calculation of amino-oxo tautomer.

Besides, the interconversion between the tautomers of 1,5-dimethylcytosine has been studied. The reaction paths connecting the structures I and III along the three transition states found (TS1, TS2 and TS3) can be noted as follows (see Fig. 5):



The structures of the TS1, TS2 and TS3 transition states can be seen in Fig. 6. The BLYP/6-31G* energies and the calculated

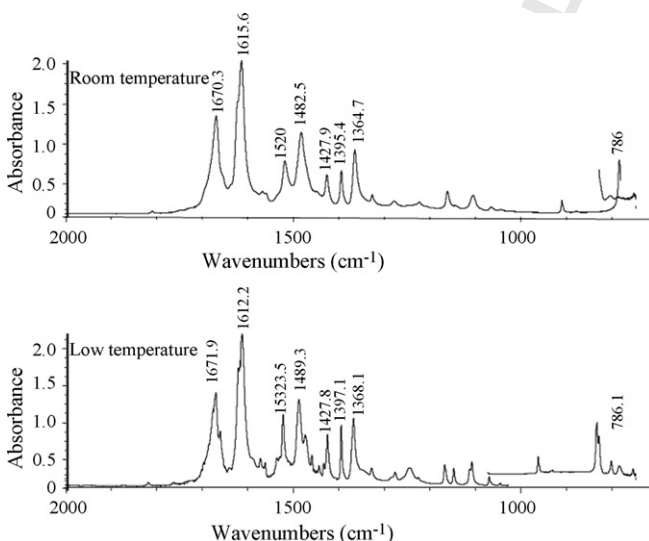


Fig. 2. The IR spectra of solid 1,5-dimethylcytosine at room temperature and at low temperature, between 2000 and 400 cm⁻¹.

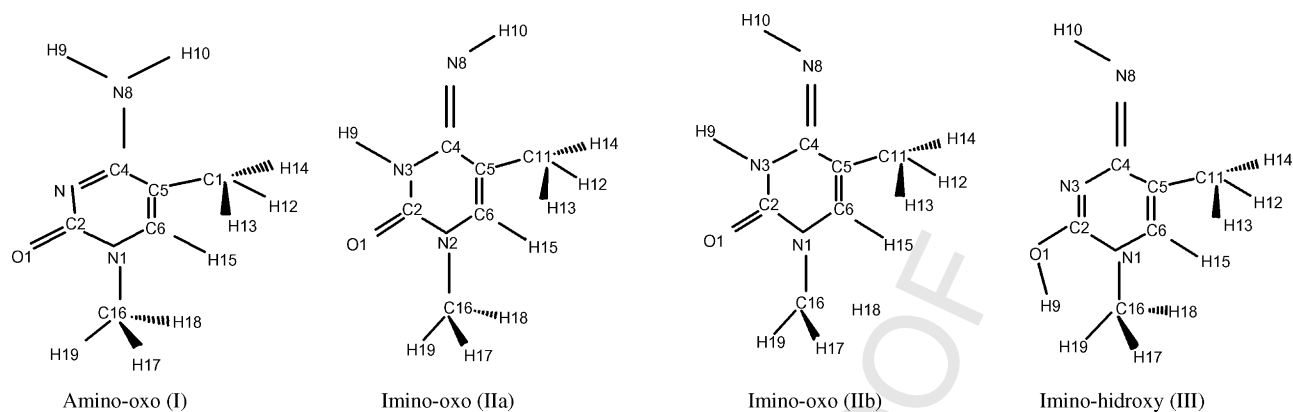


Fig. 4. Tautomers of 1,5-dimethylcytosine and atom numbering.

dipolar moment of the different structures of 1,5-dimethylcytosine are presented in Table 3.

The I, IIa and IIb tautomers are energetically very close. They are the most stable, while the III tautomer has the highest relative energy (29.1 kcal/mol). Nevertheless, the higher value of the dipolar moment of structure III would justify its existence in spite of its larger relative energy. This same behaviour has been observed by Sambrano et al. [16] for the M4 tautomer of 5-methylcytosine. TS1 and TS3 transition states correspond

with an intramolecular H9 transfer between N8 and N3 and N3 and O7, respectively. TS2 is associated with the out-of-plane deformation of the H10 atom of the imino-oxo tautomer. The normal mode of TS3 with imaginary frequency is related to the deformation of the C2O7H9 angle that connects the structures of the tautomeric forms IIb and III. The TS1 transition state connects the structures I and IIa, and is related to the deformation of the C4N3H9 angle as well as to the N8H9 stretching. The large relative energies of TS1 and TS3 (see

Table 1
Calculated B3LYP and BLYP energies (in Hartrees/molec.) for three tautomers of 1,5-dimethylcytosine

Methods	Basis	Tautomers			
		Amino-oxo	Imino-oxo(a)	Imino-oxo(b)	Imino-hidroxy
B3LYP	6-31G	−473.41408	−473.41141	−473.40973	−473.35723
	6-31G*	−473.55845	−473.55621	−473.55461	−473.51153
	6-31+G*	−473.57943	−473.57649	−473.57462	−473.53241
	6-311G**	−473.68262	−473.68649	−473.67918	−473.63880
BLYP	6-31G	−473.25897	−473.25609	−473.25463	−473.20308
	6-31G*	−473.38852	−473.38610	−473.38467	−473.34214
	6-31+G*	−473.41438	−473.41121	−473.40951	−473.36789
	6-311G**	−473.52658	−473.52526	−473.52373	−473.48265

Table 2
Averages of the differences between experimental and theoretical vibrational frequencies at different levels of theory for the amino-oxo tautomer of 1,5-dimethylcytosine

	3-21G*	6-31G	6-31+G	6-31G*	6-31+G*	6-31++G	6-31++G*	6-311G	6-311+G	6-311G*	6-311G**
BLYP											
Average	35.6	35.6	34.4	30.5	30.6	34.5	30.7	34.5	34.7	30.8	32.6
RMSD	20.8	24.9	22.8	17.6	18.3	22.8	18.3	21.7	22.4	19.5	19.5
Realibility coefficient	0.99	0.99	0.99	0.99	0.99	0.99	0.99	0.99	0.99	0.99	0.99
B3LYP											
Average	51.6	54.6	50.8	50.7	49.74	52.7	48.6	46.3	44.5	46.9	40.1
RMSD	44.6	55.6	53.9	49.5	56.62	54.7	47.4	48.1	46.4	46.8	37.7
Realibility coefficient	0.99	0.99	0.99	0.99	0.99	0.99	0.99	0.99	0.99	0.99	0.99
HF											
Average	133.6	142.4	137.9	139.1	134.0	138.3	140.0	130.0	125.6	128.2	124.4
RMSD	102.7	111.6	109.7	116.0	112.6	109.9	110.4	106.7	106.2	111.1	104.4
Realibility coefficient	0.96	0.96	0.96	0.96	0.96	0.96	0.96	0.96	0.96	0.96	0.97

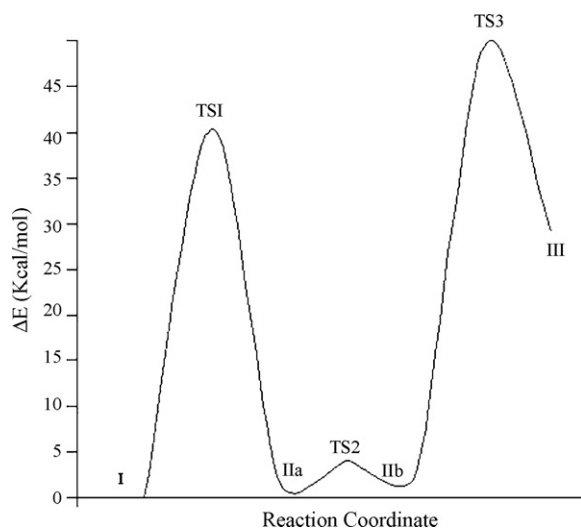


Fig. 5. Reaction path for the interconversion between the tautomers of 1,5-dimethylcytosine.

Table 3

BLYP/6-31G* total energies (E ; Hartree/molecule), relative energies (ΔE ; kcal/mol), and dipole moment (μ ; Debye) for the tautomers and the transition states connecting the minima of 1,5-dimethylcytosine

Structure	E	ΔE	μ
I	−473.38852	0.0	5.9
TS1	−473.32420	40.4	5.3
IIa	−473.38610	1.5	4.6
TS2	−473.38211	4.0	2.4
IIb	−473.38467	2.4	2.4
TS3	−473.31551	45.8	4.1
III	−473.34215	29.1	7.2

(R4,8) in the imino-oxo (1.298 Å) and the imino-hidroxy (1.301 Å) tautomers; or with the C2O7 double bond (R2,7) in the amino-oxo form (1.235 Å) that is a single bond (1.374 Å) in the imino-hidroxy tautomer. In the particular case of amino-oxo, the values of the dihedral angles τ ; (N3, C4, N8, H9) and τ ; (N3, C4, N8, H10) equals 13.4° and 156.3°, respectively, indicate that the two H atoms of the amino group are located on the same side and out of the ring plane. The torsion angles τ ; (N8, C4, C5, C11) and τ ; (O7, C2, N1, C16) are close to 0° in almost all the tautomers. On the value of torsion angle τ ; (N1C2O7H9) in tautomer III is 13.8° which indicates that the H9 atom is clearly displaced out of the ring plane.

4. Vibrational spectrum

1,5-Dimethylcytosine has 51 normal modes of vibration, all of them are active in infrared and Raman since the molecule does not possess any element of symmetry. The assignment of the vibrational spectra has been performed without taking into account possible intra and intermolecular interactions, on the basis of the BLYP/6-31G* force field and the published assignments of cytosine [3,4,10,12–14], 1-methylcytosine [11], 5-methylcytosine [13,16] and related molecules like phenylsilane, toluene, benzonitrile, phenylacetylene and aniline [28–

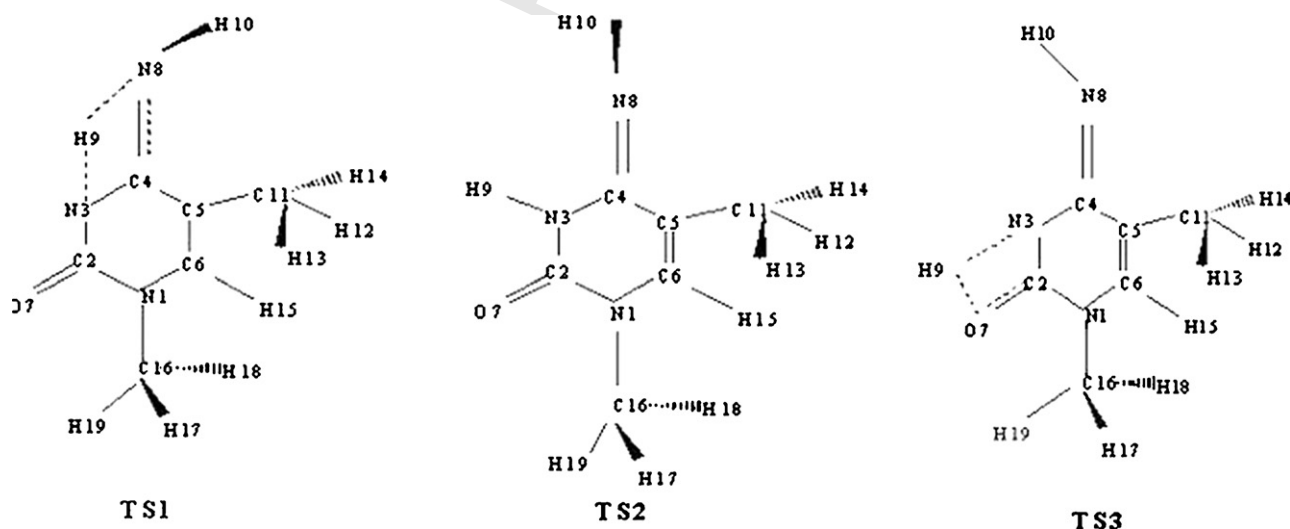


Fig. 6. Transition states for the interconversion between tautomers of 1,5-dimethylcytosine. TS1 connecting I and II, TS2 connecting IIa and IIb and TS3 connecting IIb and III tautomers, respectively (see Figs. 4 and 5).

Table 4

BLYP/6-31G* optimised geometrical parameters (*R*: bond lengths in Å; *A*: angles and *D*: dihedral angles in degrees) for the 1,5-dimethylcytosine tautomers compared with the geometrical parameters of 1-methyl and 5-methyl cytosine

Parameters	Amino-oxo	Imino-oxo IIa	Imino-oxo IIb	Imino-hidroxy III	1-Methyl-cytosine [27]	5-Methyl-cytosine [29]
<i>R</i> (1,2)	1.459	1.408	1.418	1.399	1.395	1.376
<i>R</i> (1,6)	1.367	1.398	1.392	1.412	1.357	1.365
<i>R</i> (1,16)	1.472	1.473	1.472	1.469	1.464	
<i>R</i> (2,3)	1.380	1.401	1.390	1.294	1.358	1.354
<i>R</i> (2,7)	1.235	1.234	1.234	1.374	1.234	1.252
<i>R</i> (3,4)	1.332	1.423	1.417	1.419	1.332	1.338
<i>R</i> (3,9)		1.021	1.021			
<i>R</i> (4,5)	1.450	1.471	1.473	1.482	1.422	1.438
<i>R</i> (4,8)	1.384	1.298	1.298	1.301	1.336	1.337
<i>R</i> (5,6)	1.377	1.362	1.365	1.359	1.334	1.350
<i>R</i> (5,11)	1.514	1.510	1.512	1.509		1.508
<i>R</i> (6,15)	1.094	1.092	1.093	1.092		
<i>R</i> (7,9)				0.980		
<i>R</i> (8,9)	1.020					
<i>R</i> (8,10)	1.018	1.035	1.031	1.035		
<i>R</i> (11,12)	1.102	1.102	1.101	1.103		
<i>R</i> (11,13)	1.108	1.103	1.106	1.103		
<i>R</i> (11,14)	1.106	1.103	1.106	1.103		
<i>R</i> (16,17)	1.099	1.103	1.102	1.107		
<i>R</i> (16,18)	1.101	1.103	1.102	1.098		
<i>R</i> (16,19)	1.101	1.096	1.096	1.104		
<i>A</i> (2,1,6)	121.2	121.3	121.2	116.4	120.1	121.3
<i>A</i> (2,1,16)	116.6	118.5	118.4	122.8	118.5	
<i>A</i> (6,1,16)	122.3	120.2	120.4	120.8	121.5	
<i>A</i> (1,2,3)	116.6	113.4	113.4	125.4	118.0	119.2
<i>A</i> (1,2,7)	117.9	124.1	123.3	117.2	118.6	119.0
<i>A</i> (3,2,7)	125.4	122.4	123.2	117.4	122.4	121.8
<i>A</i> (2,3,4)	120.6	128.8	129.1	120.1	120.0	119.5
<i>A</i> (2,3,9)		112.8	115.2			
<i>A</i> (4,3,9)		118.3	115.7			
<i>A</i> (3,4,5)	124.5	113.4	113.6	117.4	121.8	123.1
<i>A</i> (3,4,8)	116.3	125.2	116.5	123.0	117.8	117.1
<i>A</i> (5,4,8)	119.1	121.3	129.8	119.5	120.4	119.9
<i>A</i> (4,5,6)	114.7	118.6	118.4	118.4	117.2	115.2
<i>A</i> (4,5,11)	122.8	118.6	119.4	119.2		122.6
<i>A</i> (6,5,11)	122.4	122.8	122.2	122.4		122.2
<i>A</i> (1,6,5)	122.2	124.3	124.3	122.2	121.8	121.7
<i>A</i> (1,6,15)	116.2	114.2	114.3	114.7		
<i>A</i> (5,6,15)	121.6	121.4	121.4	123.1		
<i>A</i> (2,7,9)				110.6		
<i>A</i> (4,8,9)	114.4					
<i>A</i> (4,8,10)	118.9	111.2	109.9	107.9		
<i>A</i> (9,8,10)	115.9					
<i>A</i> (5,11,12)	110.9	111.2	111.1	111.8		
<i>A</i> (5,11,13)	112.3	110.8	111.6	110.4		
<i>A</i> (5,11,14)	111.8	110.8	111.6	110.4		
<i>A</i> (12,11,13)	106.9	108.8	107.7	109.0		
<i>A</i> (12,11,14)	107.5	108.8	107.7	109.0		
<i>A</i> (13,11,14)	107.0	106.2	106.9	105.9		
<i>A</i> (1,16,17)	109.1	110.4	110.5	111.9		
<i>A</i> (1,16,18)	109.9	110.4	110.5	108.7		
<i>A</i> (1,16,19)	109.9	107.4	107.3	111.3		
<i>A</i> (17,16,18)	110.0	109.2	109.2	107.4		
<i>A</i> (17,16,19)	110.0	109.6	109.6	109.4		
<i>A</i> (18,16,19)	107.7	109.6	109.6	107.9		
<i>D</i> (3,4,8,9)	13.4	−0.03				
<i>D</i> (3,4,8,10)	156.3	0.008	179.9	−0.4		
<i>D</i> (8,4,5,11)	1.9	−0.01	−0.004	0.9		
<i>D</i> (7,2,1,16)	0.004	−0.01	−0.011	2.9		

Table 5
BLYP/6-31G* calculated wavenumbers (cm⁻¹) and assignments of the calculated vibrational spectra of the tautomers of 1,5-dimethylcytosine

Q1

Amino-oxo		Imino-oxo IIa		Imino-oxo IIb		Imino-hidroxy	
3579.6	ν_s NH ₂	3487.8	ν N3-H9	3493.3	ν N3-H9	3607.5	ν O7-H9
3463.1	ν_a NH ₂	3298.5	ν N8-H10	3362.1	ν N8-H10	3303.1	ν N8-H10
3106.9	ν C6-H15	3129.9	ν C6-H15	3120.4	ν C6-H15	3134.8	ν C6-H15
3074.9	ν_a C16-H ₃	3110.6	ν_a C16-H ₃	3111.1	ν_a C16-H ₃	3074.3	ν_a C16-H ₃
3057.4	ν_a C16-H ₃	3044.6	ν_a C11-H ₃	3043.7	ν_a C11-H ₃	3039.6	ν_a C11-H ₃
3033.6	ν_a C11-H ₃	3026.7	ν_a C16-H ₃	3027.4	ν_a C16-H ₃	3025.9	ν_a C11-H ₃
2992.4	ν_s C16-H ₃	3023.3	ν_a C11-H ₃	2992.9	ν_a C11-H ₃	2996.7	ν_a C16-H ₃
2981.5	ν_a C11-H ₃	2975.0	ν_s C16-H ₃	2975.3	ν_s C16-H ₃	2971.1	ν_s C11-H ₃
2937.8	ν_s C11-H ₃	2973.1	ν_s C11-H ₃	2953.4	ν_s C11-H ₃	2941.1	ν_s C16-H ₃
1714.2	ν C2=O7	1730.6	ν C2=O7	1736.2	ν C2=O7	1674.7	ν C5=C6
1650.5	ν C5=C6	1661.2	ν C5=C6	1658.9	ν C5=C6	1614.6	ν C2=N3
1610.3	δ NH ₂	1621.5	ν C4=N8	1606.9	ν C4=N8	1582.3	ν C4=N8
1511.2	ν N3=C4	1496.9	δ_a C16-H ₃	1496.8	δ_a C16-H ₃	1506.5	δ_a C16-H ₃
1496.2	δ_a C16-H ₃	1493.7	δ_a C16-H ₃	1494.3	δ_a C16-H ₃	1482.3	δ_a C16-H ₃
1485.3	δ_a C11-H ₃	1486.2	δ_a C11-H ₃	1492.9	δ_a C11-H ₃	1480.2	δ_a C11-H ₃
1474.8	δ_a C11-H ₃	1461.5	δ_a C11-H ₃	1470.1	δ_a C11-H ₃	1456.6	δ_a C11-H ₃
1455.6	δ_a C16-H ₃	1426.4	δ_s C16-H ₃	1426.5	ν C4-C5	1450.6	δ_s C16-H ₃
1447.5	ν C4-N8	1416.3	ν C4-C5	1424.8	δ_s C16-H ₃	1405.3	δ_s C11-H ₃
1431.9	δ_s C16-H ₃	1410.0	δ_s C11-H ₃	1409.4	δ_s C11-H ₃	1398.8	ν C4-C5
1405.4	δ_s C11-H ₃	1380.2	β N3-H9	1371.2	β N3-H9	1357.6	ν N1-C2
1364.4	ν N1-C6	1358.3	β C6-H15	1354.5	β C6-H15	1300.6	ν C5-C11
1312.5	β C6-H15			1308.5	ν N1-C6	1273.5	ν N1-C6
1229.5	ν C5-C11	1303.5	ν N1-C6	1252.4	β N8-H10	1224.2	ν N1-C16
1182.4	ν C2-N3	1230.8	ν N1-C16	1216.5	ν C2-N3	1207.1	ν C2-O7
1125.4	ρ C16-H ₃	1202.9	ν C2-N3	1150.2	ν C5-C11	1130.8	β C6-H15
1122.8	ρ C16-H ₃	1143.1	ρ C16-H ₃	1132.6	ρ C16-H ₃	1114.4	ρ C16-H ₃
1055.5	ρ NH ₂	1133.2	ρ C16-H ₃	1094.9	ν N3=C4	1075.5	ν N3=C4
1050.2	ρ C11-H ₃	1091.9	ν N3=C4	1051.1	ρ C11-H ₃	1048.8	ρ C11-H ₃
1020.7	ν N1-C16	1053.9	ρ C11-H ₃	1041.8	ρ C16-H ₃	1033.3	ρ C16-H ₃
1004.7	ρ C11-H ₃	1043.2	ν C5-C11	999.3	ρ C11-H ₃	999.2	ρ C11-H ₃
878.2	γ C6-H15	1003.7	ρ C11-H ₃	864.6	γ C6-H15	868.3	γ N8-H10
812.9	ν N1-C2	858.5	γ C6-H15	818.9	ν N1-C2	838.7	β R ₁
736.4	β R ₁	831.1	ν N1-C2	774.1	τ N8-H10	814.2	γ C6-H15
727.1	γ O7=C2	793.9	γ N8-H10	753.5	β R ₁	733.4	β R ₃
711.3	γ N8-C4	757.1	β R ₁	704.4	γ N8-C4	712.7	γ C4-N8
659.4	ν C4-C5	706.2	γ N8-C4	697.9	γ O7=C2	658.5	β R ₂
603.4	β C2=O7	694.7	γ O7=C2	675.1	β R ₃	651.7	γ O7=C2
550.2	γ N8-H9	677.1	β R ₃	643.4	γ N3-H9	593.4	β C2=O7
521.8	β R ₂	610.3	β C2=O7	603.7	β C2=O7	510.9	τ R ₁
448.6	β R ₃	586.8	γ N3-H9	515.5	β R ₂	445.0	τ R ₃
405.8	τ R ₁	504.6	β R ₂	426.7	τ R ₁	400.6	τ C4N8-H10
392.6	γ N8-H10	427.6	τ R ₁	390.6	τ N3-H9	365.8	β C4-N8
361.9	β C4-N8	394.7	τ N3-H9	381.9	β C4-N8	344.0	β N1-C16
319.3	β N1-C16	378.6	β C4-N8	333.2	β N1-C16	312.9	γ N1-C16
280.3	γ C11-C5	330.9	β N1-C16	298.9	γ C5-C11	276.9	β C5-C11
273.8	β C5-C11	304.4	γ C5-C11	277.6	β C5-C11	236.8	γ O7-H9
225.2	τ R ₃	274.9	β C5-C11	189.6	τ_{tw} C11-H ₃	192.9	τ R ₂
188.3	τ_{tw} 11-H ₃	186.6	γ N1-C16	177.6	γ N1-C16	173.7	T_{wist} C11-H ₃
155.7	γ N1-C16	168.5	τ_{tw} C11-H ₃	126.5	τ R ₃	116.6	T_{wist} C16-H ₃
101.9	τ_{tw} C16-H ₃	125.2	τ R ₃	91.9	τ R ₂	101.3	γ C5-C11
77.3	τ R ₂	93.7	τ R ₂	64.5	τ_{tw} C16-H ₃	46.1	τ C16NIC2O7
		72.4	(τ_{tw} C16-H ₃)				

Abbreviations: ν : stretching, δ : bending, ρ : rocking, γ : wagging, τ : torsion, β : in plane deformation, τ_{tw} : twisting, β_R : deformation of the ring, τ_R : torsion of the ring, a: antisymmetric, s: symmetric.

32]. The very close energies of the amino-oxo and the imino-oxo, IIa and IIb forms, could indicate that all of them are present in the spectrum, which would complicate the discussion of the results. The calculated wavenumbers for the four tautomers of 1,5-dimethylcytosine (Table 5) have been compared with the experimental values. The wavenumbers

of the bands registered in the infrared spectra at room and at low temperature and in the Raman spectra are shown in Table 6. Although the different isomers have many calculated wavenumbers with similar values, it can be verified that the amino-oxo frequencies correspond better with the strongest and well-defined experimental bands. For this reason the assignments in

Table 6

BLYP/6-31G* wavenumbers (cm^{-1}) and assignments of the calculated vibrational spectra of tautomers of 1,5-dimethylcytosine

IR room temperature	IR low temperature	RAMAN	Assignments
3546 sh	3418 sh	3539 vw	$\nu_a \text{NH}_2$
3391 vs	3374.1 vs	3371 m	$\nu_s \text{NH}_2$
3305.8 w	3302.9 w	3300 vvw	$2 \times 919.7 + 1482.5 = 3304$
3229 vw	3231.8 w	3267 vw	$2 \times 1274 + 703 = 3251$
3112.4 m	3140 sh	3252 vvw	$2 \times 1615.6 = 3231.2$
2990 vw	3103.8 s		$4 \times 786 = 3144$
2964.4 vw	2990 vw	3114 vw	νC6H15
2933.1	2967.3 vw	3043 m	$\nu_a \text{C16H}_3$
2862.0 vvw	2935.9	3004 w	$\nu_a \text{C16H}_3$
2765.3	2864.0 vvw	2978 m	$\nu_a \text{C11H}_3$
1813 vvw	2773.8 vvw	2951 m	$\nu_s \text{C16H}_3$
1670.3 s	2756.7 vvw	2943 m	$\nu_a \text{C11H}_3$
1660 sh	1677.1 sh	2924 s	$\nu_s \text{C11H}_3$
1620.8 sh	1671.9 s	2866	$2 \times 1428 = 2856$
1615.6 vs	1660 m	2829	$2 \times 703 + 1425 = 2831$
1590 sh	1622.5 s	1656 vw	$1670.3 + 2 \times 552 = 2774.3$
1571.3 vw	1612.2 vs	1592 m	$2 \times 703 + 1364.7 = 2770.7$
1559.3 vw	1590 sh	1513 w	$1274 + 552 = 1826$
1520 m	1571.3 w	1460 w	$\nu \text{C2=O7}$
1482.5 s	1564.4 w	1425 w	$\nu \text{C5=C6}$
1464.4 sh	1550 vw	1391 m	δNH_2
1445 sh	1523.5 m	1357 w	?
1427.9 m	1489.3 s	1325 w	$2 \times 786 = 1572$
1395.4 m	1475.7 w	1274 s	δNH_2
1364.7 m	1460.3 w	1222 m	$2 \times 775 = 1550$
1328.9 w	1451 vvw	1169 w	$\nu \text{N3=C4}$
1281 vw	1445 vw	1060 w	$\nu \text{C4-N8}$
1274 sh	1434.7 vvw	1022 vw	$\delta_a \text{C16H}_3$
1224.7 vw	1427.8 w	907 vw	$\delta_a \text{C11H}_3$
1163.3 w	1397.1 s	867 m	$\delta_a \text{C11H}_3$
1147.9 sh	1368.1 s	786 w	?
1106.9 w	1349.4 sh	775 vs	$\delta_a \text{C16H}_3$
1066 vvw	1328.9 vw	750 w	?
1045.5 vvw	1284.5 sh	703 s	$\nu \text{C4-N8}$
910.7 w	1274.2 vw	624 w	$\delta_s \text{C16H}_3$
878sh	1245.2 vw	552 vs	$\delta_s \text{C11H}_3$
786 m	1224.7 vw	541 sh	?
758.7 vvw	1170.1 w	470 w	$\nu \text{N1-C6}$
741.7 vvw	1147.9 w	457 vw	βC6H15
705.8 vvw	1113.8 sh	427 w	$\nu \text{C5-C11}$
	1110.4 w	400 vw	$703 + 552 = 1255$
	1071.1 w	360 vw	$\nu \text{C2-N3}$
	1045.5 vvw	326 w	$\nu \text{C5-C11}$
	1026.7 vvw	304 w	ρC16H_3
	915.8 w	209	ρC16H_3
	883.3 vvw	183	ρNH_2
	786.1 m	165	ρC11H_3
	779.2 w	139	$\nu \text{N1-C16}$
	755.3 w	90	ρC11H_3
	736.5 w		γC6H15
	707.5 w		$\nu \text{N1-C2}$
			βR_1
			$\nu \text{C4-C5}$
			$\gamma \text{C2=O7}$
			$\gamma \text{C4-N8}$
			$\nu \text{C4-C5}$
			$\gamma \text{C4-N8}$
			$\beta \text{C2=O7}$
			γN8H9
			βR_2
			βR_3
			τR_1

Table 6 (Continued)

IR room temperature	IR low temperature	RAMAN	Assignments
			γN8H10
			$\beta \text{C4-N8}$
			βN1C16
			$\gamma \text{C5 C11}$
			$\beta \text{C5 C11}$
			τR_3
			$\tau_{\text{tw}} \text{C11H}_3$
			γN1C16
			$\tau_{\text{tw}} \text{C16H}_3$
			τR_2

Abbreviations: ν : stretching, δ : bending, ρ : rocking, γ : wagging, τ : torsion, β : in plane deformation, β_R : deformation of the ring, τ_R : torsion of the ring, τ_w : twisting, a: antisymmetric, s: symmetric, vs: very strong, s: strong, m: medium, w: weak, vw: very weak, vvw: very very weak, sh: shoulder.

Table 5 correspond with this isomer, which is the most stable as theoretical calculations predict. No evidences have been found of the significant presence of more than one tautomeric form.

4.1. 4000–2000 cm^{-1} region

In this region, the vibrational spectra show characteristic bands of normal modes related to the antisymmetric and symmetric stretchings of the N–H and C–H bonds of the amino and methyl groups, respectively, as well as the C–H stretching modes of the ring.

The shoulder and the band recorded in the room temperature infrared spectrum at 3546 and 3391 cm^{-1} , respectively, are assigned to antisymmetric and symmetric NH_2 stretching respectively. In the Raman spectrum the strongest band is located at 3371 cm^{-1} and is assigned to the symmetric stretching mode. The calculated wavenumbers for 1,5-dimethylcytosine and cytosine [3,4,10,14], 1-methylcytosine [11], 5-methylcytosine [13] and aniline [32] are in the same order. In this case the effect of anharmonicity is not so evident as in others molecules [33].

The broad, medium intensity band located at 3112.4 cm^{-1} in the room temperature infrared spectrum is recorded stronger at 3103.8 cm^{-1} in the spectrum at low temperature and is assigned to the C6–H15 stretching mode of the ring. In the Raman spectrum this last band is recorded very weak at 3114 cm^{-1} .

The Raman bands at 3043, 3004, 2978, 2951, 2943 and 2924 cm^{-1} are assigned to antisymmetric and symmetric C–H stretching of both methyl groups. The order of the assignments is summarised in Table 6. In the Raman spectrum the strongest bands at 2951 and 2924 cm^{-1} are assigned to symmetric stretching modes corresponding to both CH_3 groups.

4.2. 1700–1500 cm^{-1} region

In this region the C=OR, C=C and C–N stretching modes, as well as the NH_2 deformation are expected. The characteristic strong infrared band recorded at 1670.3 cm^{-1} at room temperature is assigned to the C2=O7 stretching mode. This band is split in two bands at 1677.1 cm^{-1} and 1671.9 cm^{-1} in

the spectrum at low temperature, like in cytosine [14] and 5-methylcytosine [13]. This splitting could be attributed to a possible Fermi resonance as occurs in cytosine tautomers [12]. In the amino-oxo tautomer of 5-methylcytosine [13] this vibration is observed at 1735 cm^{-1} whereas in the same tautomer of cytosine is observed at 1719 and 1733 cm^{-1} [12].

The shoulder recorded in infrared at 1660 cm^{-1} shows a significant intensity, and is assigned to the C5=C6 stretching mode. The calculated wavenumber for this fundamental mode is 1650.5 cm^{-1} .

The strong band at 1615.6 cm^{-1} is observed sharp and with stronger intensity in the low temperature spectrum, it being assigned to the NH_2 deformation. This mode was observed at 1703 cm^{-1} [3], 1749 cm^{-1} [4], 1595 cm^{-1} [10], 1598 cm^{-1} [14] in amino-oxo tautomer of cytosine and at 1592 cm^{-1} in 1-methylcytosine [11] and at 1595 cm^{-1} in 5-methylcytosine [13], while it is observed at 1618 cm^{-1} in the spectrum of aniline [32]. The calculated wavenumber for this deformation mode using HF/3-21G method is 1628 cm^{-1} in 5-methylcytosine [13] and 1579 cm^{-1} using CNDO/2 FORCE method in 1-methylcytosine [11]. In 1,5-dimethylcytosine this mode is calculated at 1610.3 cm^{-1} . It is the strongest one of the Raman spectrum where it is recorded at 1592 cm^{-1} . The shoulder at 1590 cm^{-1} in the infrared and Raman spectra remains unassigned. In the case of amino-oxo form of cytosine [10,12] the band at 1599 cm^{-1} is assigned to the scissoring motion. In addition, splitting is observed in the spectrum at low temperature (1571.3 and 1564.4 cm^{-1}) for the band at room temperature 1571.3 cm^{-1} due to combinations in possible Fermi resonance with the fundamentals.

The medium intensity band recorded in the room temperature infrared spectrum at 1520 cm^{-1} and at 1523.5 cm^{-1} in the low temperature spectrum is assigned to the N3=C4 stretching.

4.3. $1500\text{--}1000\text{ cm}^{-1}$ region

The majority of the bands in this region are due to deformation modes of the CH_3 groups and to stretching C–C and C–N bonds too. In this zone the theoretical calculations predict the frequencies and the intensities of the bands accurately for which permits to carry out a reliable assignment, as is observed in Fig. 7 compared with the experimental spectrum. Many of this bands appear split in two at low temperature (e.g. doublets: 1489.3 and 1475.7 ; 1460.3 and 1451 ; 1445 and 1434.7 ; 1368.1 and 1349.4 ; 1274.2 and 1245.2 ; 1113.8 and 1110.4) due to Fermi resonance as in other aromatic ring [12]. According to their characteristic intensities, the strong band recorded at 1482.5 cm^{-1} in the room temperature spectrum and at 1489.3 and 1475.7 cm^{-1} at low temperature could be assigned to the N- CH_3 or C- CH_3 antisymmetric deformation. The shoulders at 1464.4 and 1445 cm^{-1} are assigned to the remaining C- CH_3 and N- CH_3 antisymmetric deformations, respectively. The band of medium intensity in the infrared spectrum at 1427.9 cm^{-1} is assigned to the C4–N8 stretching mode.

Force field calculations predict in this region the onset of stretching vibrations of the ring, in-plane C–H deformation and

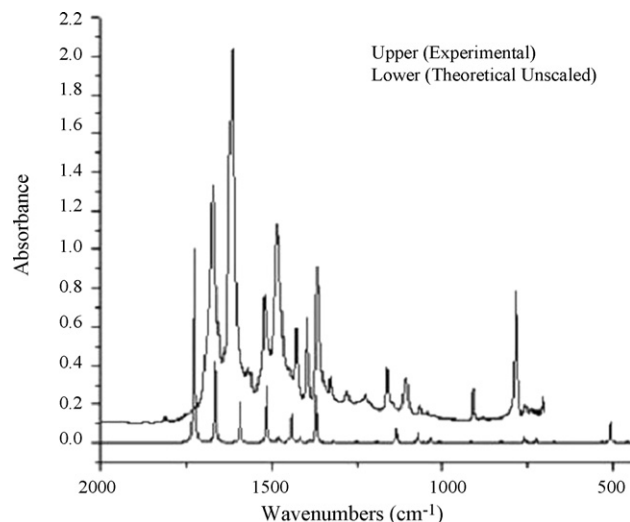


Fig. 7. The comparison IR spectra of solid 1,5-dimethylcytosine at room temperature with the theoretical spectrum between 2000 and 400 cm^{-1} .

rocking modes of both NH_2 and methyl groups. In similar molecules, like cytosine [3,4,12,14], 1-methylcytosine [11] and 5-methylcytosine [13], the same set of vibrations are observed.

The medium intensity band at 1395.4 cm^{-1} recorded in the infrared spectrum is assigned to the N- CH_3 symmetric deformation, while the band at 1364.7 cm^{-1} is assigned to C- CH_3 symmetrical deformation. The same band is observed in the Raman spectrum with very weak intensity at 1357 cm^{-1} . The 1328.9 cm^{-1} band is assigned to N1–C6 stretching while the very weak band located at 1281 cm^{-1} is assigned to the C6–H15 in-plane deformation. The theoretical spectrum predicts these modes at 1364.4 and 1312.5 cm^{-1} , respectively (see Table 5) whereas the very weak band at 1224.7 cm^{-1} is assigned to the C2–N3 stretching.

The N- CH_3 rocking modes are assigned at 1163.3 and 1147.9 cm^{-1} infrared bands because the theoretical spectrum predicts these modes at 1125.4 and 1122.8 cm^{-1} .

The NH_2 rocking is observed in cytosine [14], 1-methylcytosine [11] and 5-methylcytosine [13] at 1083 , 1142 and 1074 cm^{-1} , respectively. For this, the band at 1106.9 cm^{-1} of the room temperature spectrum, which appears split in 1113.8 and 1110.4 cm^{-1} at low temperature, is assigned to this vibration.

The N- CH_3 rocking in 1-methylcytosine [11] is observed at 1044 cm^{-1} while in the theoretical spectrum of 1,5-dimethylcytosine appear at 1055.5 cm^{-1} consequently the very weak band at 1066 cm^{-1} is assigned to this mode.

As observed in Table 5 the theoretical spectrum predicts the N1–C16 stretching of the amino-oxo tautomer at 1020.7 cm^{-1} therefore this mode is assigned to the very weak band at 1045.5 cm^{-1} .

The band recorded at 1022 cm^{-1} in the Raman spectrum and at 1026.7 cm^{-1} at low temperature is assigned to the C- CH_3 rocking. This mode in the theoretical spectrum of 1,5-dimethylcytosine is observed at 1004.7 cm^{-1} whereas in 5-methylcytosine [13] with the HF/3-21G method appear theoretically hardly coupled with the NH_2 rocking at

1074 cm⁻¹ and with greater contribution at 1006 cm⁻¹ but is observed experimentally at 998 cm⁻¹.

4.4. 1000–100 cm⁻¹ region

The assignments in this region are less reliable due to the large number of vibrations expected: ring deformations, C2=O7, C4–N8, N1–C16, C5–C11 out-of-plane deformations and, ring torsions and CH₃ and NH₂ groups torsion.

The theoretical spectrum of the amino-oxo tautomer predicts the C6H15 out-of-plane deformation at 878.2 cm⁻¹ hence, the weak band observed in the spectrum at room temperature at 910.7 cm⁻¹ is assigned to this vibrational mode.

The shoulder recorded at 878 cm⁻¹ in the infrared, observed in the Raman spectrum as an intense band at 867 cm⁻¹, is assigned to the N1–C2 stretching vibration. In the case of cytosine [14] this mode is calculated using HF/6-31G** method with greater contribution at 911 cm⁻¹ whereas in the amino-oxo tautomer of 5-methylcytosine [13] appear theoretically with HF/3-21G method at 886 cm⁻¹ and observed at 877 cm⁻¹.

The strongest infrared band of this region is observed at 786 cm⁻¹, and it is split in two bands at 786.1 and 779.2 cm⁻¹ in the spectrum at low temperature, while in the Raman spectrum only one band is observed at 775 cm⁻¹. On the basis of both, the position and the intensity, it is assigned as a deformation of the ring, such mode being calculated at 736.4 cm⁻¹. The remains deformation of the ring mode are observed at 541 and 470 cm⁻¹. In related molecules like phenylsilane this modes appear at 704, 690 and 388 cm⁻¹, in toluene at 789, 627 and 521 cm⁻¹, in benzonitrile with greater contribution are observed at 997, 752, 623 cm⁻¹ while in phenylacetylene at 998, 754 and 625 cm⁻¹ and in aniline at 990, 690 and 619 cm⁻¹ [28–32]. The significative difference between this values probably is due at to calculations they carried out with different theoretical method.

The theoretical spectrum predicts the C2=O7 out-of-plane deformation at 727.1 cm⁻¹. Thus, the very weak infrared band at 758.7 cm⁻¹ is assigned to this vibration. In the amino-oxo tautomer of cytosine this mode is calculated at 794 cm⁻¹ and is registered at 781 cm⁻¹ [14]. The calculated wavenumber of the C4–N8 out-of-plane deformation, also called NH₂ inversion mode [12], is 727.1 cm⁻¹ and it is observed at 782 cm⁻¹ in the Raman, while in the room and low temperature spectra it is recorded at 741.7 cm⁻¹ and 736.5 cm⁻¹, respectively.

The theoretical force field predicts the C4–C5 stretching mode at 659.4 cm⁻¹. Thus, the strong Raman band at 703 cm⁻¹ is assigned to this fundamental. It is calculated at 749 cm⁻¹ and observed at 747 cm⁻¹ in the amino-oxo tautomer of cytosine [14]. In the amino-oxo tautomer of 5-methylcytosine [13] is calculated at 886 cm⁻¹ and observed at 877 cm⁻¹.

The strong Raman band at 552 cm⁻¹ is assigned as N8–H9 out-of-plane deformation. This mode is calculated at 565 cm⁻¹ in the case of the amino-oxo tautomer of cytosine and observed at 525 cm⁻¹ and 520 cm⁻¹ in Argon and Neon matrices [12], respectively. This mode appear with greater contribution in the same tautomer of 5-methylcytosine [13] at 613 cm⁻¹ and is observed at 609 cm⁻¹.

The shoulder recorded in the Raman spectrum at 541 cm⁻¹ is assigned as a ring deformation. In 5-methylcytosine this mode is observed at 478 cm⁻¹ [13] while in the amino-oxo tautomer of cytosine is predicted at 526 cm⁻¹ and observed at 535 cm⁻¹ [14].

The very weak band in the Raman spectrum at 470 cm⁻¹ is assigned to the deformation of the ring because the theoretical spectrum predicts a wavenumber of 448.7 cm⁻¹.

The very weak Raman line of 457 cm⁻¹ is assigned as a torsion of the ring. In the amino-oxo tautomer of 5-methylcytosine this mode is calculated at 442 cm⁻¹ [13] whereas at 405.8 cm⁻¹ in 1,5-dimethylcytosine. In the case of the amino-oxo tautomer of cytosine it is predicted at 477 cm⁻¹ and observed at 498 cm⁻¹ [12].

The N8–H10 out-of-plane deformation is assigned to the weak Raman band recorded at 427 cm⁻¹. It is calculated at 447 cm⁻¹ in the amino-oxo tautomer of cytosine and observed at 535 cm⁻¹ and 531 cm⁻¹ in Argon and Neon matrices [12], respectively. In the amino-oxo tautomer of 5-methylcytosine it is calculated at 452 cm⁻¹ and is observed at 406 cm⁻¹ [13].

The assignments of the remaining bands in this region are shown in Table 6 and were carried out taking into account the calculated wavenumbers (see Table 5) and the assignments of the spectrum of the amino-oxo tautomers of cytosine [14] and 5-methylcytosine [13]. These bands are related to torsions of the ring and to the N-CH₃ and C-CH₃ out-of-plane modes.

5. Conclusions

Four tautomers of 1,5-dimethylcytosine have been theoretically found. According to the respective energies and the analysis of the vibrational spectra, the following stability order has been established: I > IIa > IIb > III. The respective stability could depend strongly on their intermolecular interactions, temperature and aggregation state as previously observed in 5-methylcytosine [16].

The high value of the potential barrier would limit the quick interconversion between the imino-oxo IIa and IIb tautomers, although the simultaneous presence of both could be justified by the close values of energies. On the other hand, the high calculated barrier for the imino-hidroxy tautomer and its high energy discard to expect a significant abundance for this form.

The theoretical level that best reproduces the experimental vibrational wavenumbers of the amino-oxo tautomer is BLYP/6-31* with a standard deviation of 17.6 cm⁻¹ and a reliability coefficient of 0.99.

The assignments of the vibrational modes of the amino-oxo (I) tautomer and the corresponding calculated wavenumbers for the four tautomers of 1,5-dimethylcytosine are reported. From the correspondence between the observed bands and the result of the calculated force field it was deduced that the most stable tautomer would be the amino-oxo (I) form.

Acknowledgements

S.A. Brandán thanks the Beca Banco Rio for a grant supporting this work. The research grants of CIUNT (Consejo

de Investigaciones de la Universidad Nacional de Tucumán, R. Argentina) and CONICET (Consejo Nacional de Investigaciones Científicas y Técnicas, R. Argentina).

References

- [1] R.J.H. Clark, R.E. Hester, *Spectroscopy of Biological Systems*, vol. 13, J. Wiley & Sons, 1986.
- [2] F. Korte (Ed.), *Methodicum Chemicum*, Vol. III Part I, Nucleic Acids, Proteins and Carbohydrates, Academic Press, New York, 1976.
- [3] H. Susi, J.S. Ard, J.M. Purcell, *Spectrochim. Acta* 29A (1973) 725.
- [4] E.D. Radchenko, G.G. Sheina, N.A. Smorygo, Y.P. Blagoi, *J. Mol. Struct.* 116 (1984) 387.
- [5] M. Mathlōthi, A.M. Seuvre, J.L. Koenig, *Carboh. Res.* 146 (1986) 1.
- [6] M. Tsuboi, S. Takahashi, I. Harada, in: J. Duchesne (Ed.), *Physico Chemical Properties of Nucleic Acids*, vol. 2, Academic Press, New York, 1973.
- [7] S. Aruna, G. Sahnugam, *J. Raman Spectrosc.* 16 (4) (1985) 229.
- [8] R. Letellier, M. Ghomi, E. Taillandier, *Eur. Biophys. J.* 14 (1987) 227.
- [9] P. Lagant, P. Derreumaux, G. Vergoten, W. Peticolas, *J. Comp. Chem.* 12 (6) (1991) 731.
- [10] M. Szczesniak, K. Szczepaniak, J.S. Kwiatkowski, K. KuBulat, W.B. Person, *J. Am. Chem. Soc.* 110 (1988) 8319.
- [11] K. Kuczera, M. Szczesniak, K. Szczepaniak, *J. Mol. Struct.* 172 (1988) 73.
- [12] M.J. Nowak, L. Lapinski, J. Fulara, *Spectrochim. Acta* 45A (2) (1989) 229.
- [13] L. Lapinski, M.J. Nowak, J. Fulara, A. Lés, L. Adamowicz, *J. Phys. Chem.* 94 (1990) 6555.
- [14] I.R. Gould, M.A. Vincent, I.H. Hillier, L. Lapinski, M.J. Nowak, *Spectrochim. Acta* 48A (6) (1992) 811.
- [15] H. Rostkowska, M.J. Nowak, L. Lapinski, M. Bretner, T. Kulikowski, A. Lés, L. Adamowicz, *Spectrochim. Acta* 49A (4) (1993) 551.
- [16] J.R. Sambrano, A.R. de Souza, J.J. Queralto, M. Oliva, J. Andrés, *Chem. Phys.* 264 (2001) 333.
- [17] S. Sánchez-Cortes, J.V. García-Ramos, *J. Raman Spectrosc.* 21 (1990) 679.
- [18] S. Sánchez-Cortes, J.V. García-Ramos, *Langmuir* 16 (2000) 764.
- [19] G. Vilkaitis, I. Suetake, S. Klimasauskas, S. Tajima, *J. Biol. Chem.* 280 (1) (2005) 64.
- [20] E. Merkiene, S. Klimasauskas, *Nucleic Acids Res.* 33 (1) (2005) 307.
- [21] S. Klimasauskas, R. Gerasimaite, G. Vilkaitis, S. Kulakauskas, *Nucleic Acids Symp. Ser.* 2 (1) (2002) 73.
- [22] M.J. Frisch, G.W. Trucks, H.B. Schlegel, G.E. Scuseria, M.A. Robb, J.R. Cheeseman, V.G. Zakrzewski, J.A. Montgomery Jr., R.E. Stratmann, J.C. Burant, S. Dapprich, J.M. Millam, A.D. Daniels, K.N. Kudin, M.C. Strain, O. Farkas, J. Tomasi, V. Barone, M. Cossi, R. Cammi, B. Mennucci, C. Pomelli, C. Adamo, S. Clifford, J. Ochterski, G.A. Petersson, P.Y. Ayala, Q. Cui, K. Morokuma, D.K. Malick, A.D. Rabuck, K. Raghavachari, J.B. Foresman, J. Cioslowski, J.V. Ortiz, A.G. Baboul, B.B. Stefanov, G. Liu, A. Liashenko, P. Piskorz, I. Komaromi, R. Gomperts, R.L. Martin, D.J. Fox, T. Keith, M.A. Al-Laham, C.Y. Peng, A. Nanayakkara, C. Gonzalez, M. Challacombe, P.M.W. Gill, B. Johnson, W. Chen, M.W. Wong, J.L. Andres, C. Gonzalez, M. Head-Gordon, E.S. Replogle, J.A. Pople, *Program GAUSSIAN 98*, revision A.7, Gaussian, Inc., Pittsburgh, PA, USA, 1998.
- [23] P.S. Levy, S. Lemeshow, *Sampling of Populations Methods and Applications*, John Wiley & Sons, Inc., New York, 1999.
- [24] B. Trus, R. Marsh, *Acta Cryst.* B28 (1972) 1834.
- [25] M. Rossi, T.J. Kistenmacher, *Acta Cryst.* B33 (1977) 3962.
- [26] A. Takenaka, M. Kato, Y. Sasada, *Bull. Chem. Soc. Jpn.* 53 (1980) 383.
- [27] C.T. Grainger, D. Bailey, *Acta Cryst.* B37 (1981) 1561.
- [28] M. Alcolea Palafox, *Recent Res. Dev. Phys. Chem.* 2 (1998) 213.
- [29] Y. Xie, J. Boggs, *J. Comput. Chem.* 7 (2) (1986) 158.
- [30] A.G. Császár, G. Fogarasi, *Spectrochim. Acta* 45A (8) (1988) 845.
- [31] A.G. Császár, G. Fogarasi, J.E. Boggs, *J. Phys. Chem.* 93 (1989) 7644.
- [32] Z. Niu, K.M. Dunn, J.E. Boggs, *Mol. Phys.* 55 (2) (1985) 421.
- [33] P. Pulay, G. Fogarasi, G. Pongor, J.E. Boggs, A. Vargha, *J. Am. Chem. Soc.* 105 (24) (1983) 7037.